Spectroscopic Properties, Electrochemistry, and Reactivity of Mo^0, Mo^I, and Mo^{II} Complexes with the [Mo(bpa)$(CO)_3$] Unit [bpa = bis(2-picolyl)amine] and Their Application for the Labelling of Peptides

Dave R. van Staveren,[a][‡] Eberhard Bothe,[a] Thomas Weyhermüller,[a] and Nils Metzler-Nolte*[b]

Dedicated to Professor Karl Wieghardt on the occasion of his 60th birthday

Keywords: Amino acids / Bioinorganic chemistry / Carbonyl ligands / Molybdenum / Spectro-electrochemistry

The synthesis of the complexes [Mo(bpa)$(CO)_3$] (**1**) and [Mo(Bz-bpa)$(CO)_3$] (**2**) [bpa = bis(2-picolyl)amine; Bz-bpa = *N*-benzylbis(2-picolyl)amine] is described. These compounds have been characterized by spectroscopic techniques including multinuclear NMR spectroscopy (^{1}H, ^{13}C, and ^{95}Mo), and also by X-ray crystallography. Complexes **1** and **2** underwent reversible one-electron oxidations in acetonitrile and dichloromethane with Bu_4NPF_6 as supporting electrolyte to yield the 17-electron organometallic compounds $\mathbf{1}^+$ and $\mathbf{2}^+$. With Bu_4NBr as supporting electrolyte in dichloromethane, on the other hand, **1** and **2** underwent electrochemically irreversible two-electron oxidations, resulting in the formation of [Mo(bpa)$(CO)_3$Br]$^+$ and [Mo(Bz-bpa)$(CO)_3$Br]$^+$. Infrared spectra and electronic spectra of these oxidized species were recorded in spectro-electrochemical studies. The electrochemical behaviour and the infrared spectroscopic data of **1**, **2**, and their oxidized derivatives are compared in detail with those of analogous tricarbonylmolybdenum complexes with the ligands 1,4,7-triazacyclononane and hydridotris(pyrazolyl)borate. The complex [Mo(bpa)(CO)Br]Br_3 (**3**) could be prepared by oxidation of **1** with elemental bromine. Under aerobic aqueous conditions, **3** reacted further to yield the dinuclear diamagnetic Mo^V complex [Mo_2(bpa)$_2$(O)$_2$(μ-O)$_2$](Br,PF_6) (**4**). The identity of **4** was confirmed by a single-crystal X-ray crystallographic study. Finally, the syntheses of two bioconjugates of [Mo(bpa)$(CO)_3$], in which bpa ligands are covalently linked to the *N*-termini of an amino acid (Phe-OMe, **8a**) and of a dipeptide (Ala-Phe-OMe, **8b**), are described. These bioconjugates were comprehensively characterized (including elemental analysis, ^{1}H, ^{13}C, and ^{95}Mo NMR, IR, MS, and electrochemistry). All analytical data supported the proposed constitution and underscore the potential of the Mo(bpa)$(CO)_3$ group as a robust marker group in bioorganometallic chemistry.

Introduction

There is considerable interest in the labelling of biomolecules with organometallic fragments that possess carbonyl ligands.[1−3] The corresponding bioconjugates can be detected in picomolar quantities by infrared spectroscopy, as shown by Jaouen, Salmain, and co-workers.[4] Together with IR spectroscopy, electrochemistry of metal complexes is a very attractive detection method, offering good sensitivity and a high signal-to-background ratio.[5,6] We have recently introduced the versatile and robust Mo(allyl)$(CO)_2$ moiety as a marker group in bioorganometallic chemistry.[7−9] However, perhaps the most obvious low-valent Mo fragment is *fac*-Mo$(CO)_3$, in the form of octahedral [L_3Mo$(CO)_3$] complexes. For biological applications, the ligand L_3 must fulfil several requirements. It must be readily accessible, easily substituted with a handle for biomolecules, and furnish very stable Mo$(CO)_3$ complexes. Well-known examples of [L_3Mo$(CO)_3$] complexes include L_3 = 1,4,7-triazacyclononane (tacn; [9]aneN_3) and hydridotris(pyrazolyl)borate [HB$(pz)_3$] as tridentate ligands. We propose the bis(2-picolyl)amine ligand [*bis*(*picolyl*)*amine*, bpa] as an interesting alternative, because its Mo$(CO)_3$ complexes are readily accessible and very stable, as shown here. Moreover, in contrast to tacn and hydridotrispyrazolylborate, the bpa ligand can easily be derivatized with a (protected) acid functionality,[10,11] which makes binding to biomolecules possible.[11,12]

[a] Max-Planck-Institut für Strahlenchemie,
Stiftstrasse 34−36, 45470 Mülheim/Ruhr, Germany
[b] Pharmazeutisch-Chemisches Institut, Universität Heidelberg,
Im Neuenheimer Feld 364, 69210 Heidelberg, Germany
Fax: (internat.) + 49-(0)6221/546441
E-mail: Nils.Metzler-Nolte@urz.uni-heidelberg.de
[‡] Present address: Max-Planck-Institut für Kohlenforschung,
Kaiser-Wilhelm-Platz 1, 45470 Mülheim/Ruhr, Germany
Supporting information for this article is available on the WWW under http://www.eurjic.com or from the author.

The ligand bpa, first reported by Romary et al.,[13] is one of the classical tridentate nitrogen donor ligands in coordination chemistry, but (bpa)metal complexes containing *organometallic* fragments are relatively scarce. Only four organometallic bpa complexes have so far been structurally characterized by X-ray crystallography: namely, [Rh(bpa)(cod)]BPh_4 [cod = (*Z*,*Z*)-1,5-cyclooctadiene],[14] [Pt(bpa)CH_3]Cl,[15] [Pt(bpa)(η^1-allyl)$(CH_3)_2$]Br,[15] and [W(bpa)(η^3-allyl)$(CO)_2$]PF_6.[16] A significant number of *fac*-[L_3Mo$(CO)_3$] complexes, with L_3 being a tridentate nitrogen donor ligand, have been structurally characterized.[17–34] However, no Mo(bpa)$(CO)_3$ derivatives have yet been reported. Krüger and Helm reported the synthesis and X-ray crystal structure of a related compound, in which the potentially tetradentate ligand *N*,*N*′-dimethyl-2,11-diaza-[3.3](2,6)pyridinophane acts as a tridentate ligand structurally analogous to bpa.[17]

In this paper, we report the synthesis, structural characterisation, spectroscopic properties, electrochemical behaviour and chemical reactivity of Mo^0, Mo^I, and Mo^{II} complexes containing the Mo(R-bpa)$(CO)_3$ unit (R = H or Bz). Furthermore, the suitability of Mo(R-bpa)$(CO)_3$ complexes for the labelling of biomolecules is demonstrated by the synthesis of two derivatives, an amino acid (Phe) and a dipeptide (Ala-Phe), in which the Mo(R-bpa)$(CO)_3$ derivative is covalently linked to the *N*-termini.

Results and Discussion

Synthesis and Reactivity

The complexes [Mo(bpa)$(CO)_3$] (**1**) and [Mo(Bz-bpa)$(CO)_3$] (**2**) were synthesized by heating the ligand with $Mo(CO)_6$ in deoxygenated di-*n*-butyl ether (for **1**) or deoxygenated mesitylene (for **2**) at 150 °C for 1 h under argon, as shown in Scheme 1. Complex **1** was isolated as a deep yellow powder, whereas **2** was obtained as an orange solid. All the characterisation data for **1** and **2** were consistent with their proposed constitutions. These compounds were stable in air for days in the solid state. In solution, complex **1** was much more sensitive than **2** towards air, with decomposition of **1** taking place within 1–2 h.

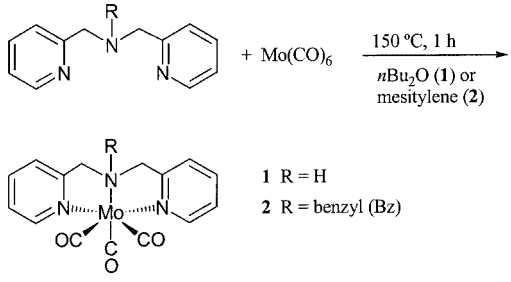

Scheme 1

When **1** was treated with elemental bromine in deoxygenated $CHCl_3$ under argon, the orange-brown complex [Mo(bpa)$(CO)_3$Br]Br_3 (**3**) was obtained (see Scheme 2), as concluded from the results of elemental analysis, infrared spectroscopy and ESI positive mass spectrometry. In the solid state, this compound was stable towards dioxygen for approximately 1 d, but in solution decarbonylation of complex **3** took place within 5–10 min when only traces of water were present. NMR spectroscopic data of compound **3** could not be obtained. When **3** was dissolved in MeOH under aerobic conditions and an aqueous solution of KPF_6 was added, the dinuclear complex [Mo_2(bpa)$_2(O)_2$(μ-$O)_2$](Br,PF_6) (**4**) invariably precipitated, and therefore appears to be the thermodynamic sink of the mixture (see Scheme 2). The reactivity of **3** differed from that of [Mo([9]aneN_3)$(CO)_3$Br]Br_3, as the latter compound can be crystallized from aerobic aqueous solutions.[35]

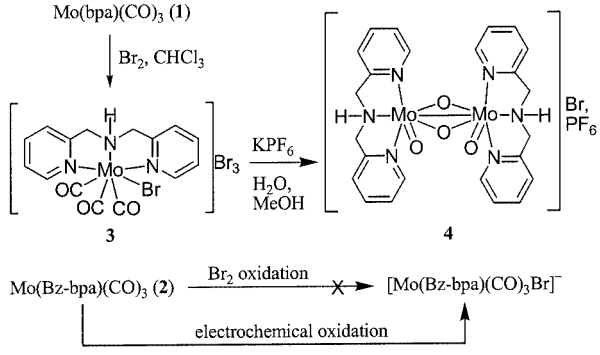

Scheme 2

When **2** was treated with Br_2 under conditions identical to those used for the synthesis of **3**, an oil formed initially, but an orange-brown solid was obtained upon removal of the solvent in vacuo. Although results from elemental analysis fitted well for [Mo(Bz-bpa)$(CO)_3$Br]Br_3, other characterisation data could not be obtained, due to the instability of this compound in solution. However, [Mo(Bz-bpa)$(CO)_3$Br]$^+$ could be generated by electrochemical methods (see Scheme 2), as concluded from spectro-electrochemical investigations (vide infra).

X-ray Crystal Structures of 1, 2, and 4

X-ray quality single crystals of complexes **1** and **2** were obtained by slow concentration of H_2O/CH_3CN solutions under streams of argon. The unit cell of each compound was found to consist of two crystallographically inequivalent molecules (named A and B), which display slightly different bond lengths and angles. ORTEP diagrams for one of the independent molecules of each of **1** and **2** are depicted in Figures 1 and 2, respectively. Geometrical information for both structures is summarized in Table 1. Molecules B of **1** and **2** are labelled consecutively: N(1) in A corresponds to N(4) in B, and C(35) in B corresponds to C(13) in A, etc. The two independent molecules in the two structures are fairly similar.

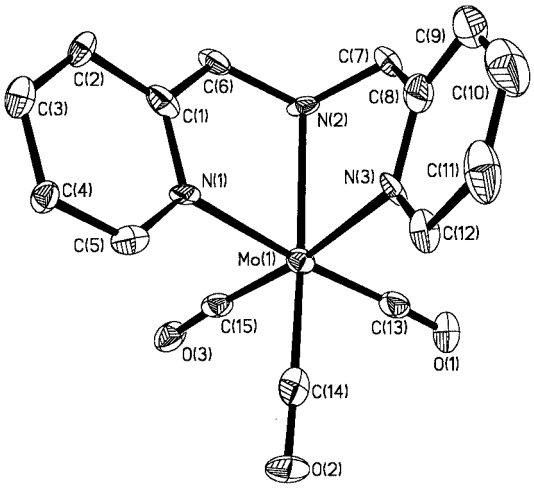

Figure 1. ORTEP projection for one of the two crystallographically independent molecules (A) of **1** with thermal ellipsoids at 50% probability level; hydrogen atoms have been omitted for clarity

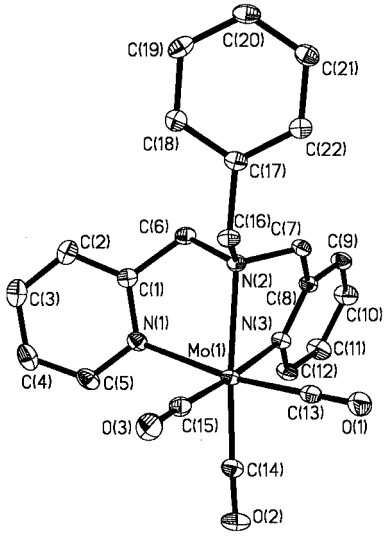

Figure 2. ORTEP plot for one of the two crystallographically independent molecules (A) of **2** with thermal ellipsoids at 50% probability level; hydrogen atoms have been omitted for clarity

The Mo atoms in both structures are in distorted octahedral $[N_3C_3]$ coordination environments, each with the three carbonyl groups and the (substituted) bis(2-picolyl)-amine ligand occupying a face of the octahedron. This facial arrangement of the carbonyl ligands has also been observed in analogous complexes with various tridentate N-donor ligands.[17−34] In both molecules of **1** and **2**, the Mo−N(amine) bond length is considerably longer than the Mo−N(pyridine) bond lengths. Unfortunately, the quality of the structure of **1** is not high enough to allow a detailed discussion of the other bond lengths in this structure. All of the differences between molecule A and molecule B of **2** are small and might be interpretable on the basis of packing effects. In both structures the deviation from idealized octahedral symmetry is evident from the C−Mo−C angles: values of less than 90° are observed for all of those. In fact,

Table 1. Selected bond lengths [Å] for $[Mo(bpa)(CO)_3]$ (**1**) and $[Mo(Bz\text{-}bpa)(CO)_3]$ (**2**)

	1	**2**
Molecule A:[a]		
Mo(1)−N(1)	2.229(10)	2.272(3)
Mo(1)−N(2)	2.301(10)	2.337(2)
Mo(1)−N(3)	2.234(11)	2.255(3)
Mo(1)−C(13)	1.92(2)	1.933(3)
Mo(1)−C(14)	1.91(2)	1.935(2)
Mo(1)−C(15)	1.91(2)	1.945(3)
Molecule B:[b]		
Mo(2)−N(4)	2.249(11)	2.250(3)
Mo(2)−N(5)	2.308(11)	2.331(2)
Mo(2)−N(6)	2.249(11)	2.252(3)
Mo(2)−C(35)	1.92(2)	1.938(3)
Mo(2)−C(36)	1.89(2)	1.932(3)
Mo(2)−C(37)	1.92(2)	1.953(3)

[a] The unit cells of both compounds contain two crystallographically independent molecules, named A and B. [b] Molecule B is labelled consecutively: i.e., N(4) in B corresponds to N(1) in A and C(35) in B corresponds to C(13) in A, etc.

all structures so far reported for *fac*-$Mo(CO)_3$ complexes with tridentate N-donor ligands display C−Mo−C angles smaller than 90°,[17−34] and this deviation thus appears to be a general feature for this type of compounds.

There is only one example in the literature of a structurally characterized *fac*-$Mo(CO)_3$ compound with the molybdenum atom coordinated by two pyridine nitrogen atoms and one amine nitrogen atom of the same ligand. The potentially tetradentate ligand *N*,*N*′-dimethyl-2,11-diaza[3.3]-(2,6)pyridinophane acts as a tridentate ligand in that compound.[17] The Mo−N(pyridine) bond lengths in the structure of that complex are approximately 0.04 Å longer than the Mo−N(amine) bond lengths. This is in sharp contrast with structures **1** and **2**, in which the Mo−N(pyridine) bond lengths are considerably shorter than the Mo−N(amine) bond lengths.

X-ray quality single crystals of $[Mo_2(bpa)_2(O)_2(\mu\text{-}O)_2](Br,PF_6)$ (**4**) were obtained by slow concentration of an $MeOH/H_2O$ solution. An ORTEP representation of the cationic part of **4** is shown in Figure 3, with selected bond length and bond angle information summarized in Table 2.

The cationic part of the structure consists of two Mo(bpa)(O) moieties bridged by two oxo ligands, with the terminal oxo ligands occupying *cis* positions relative to each other. The four-membered ring comprised of the two Mo atoms and the two bridging oxo ligands has the puckered conformation observed in all crystal structures containing a *syn*-$[Mo_2(O)_2(\mu\text{-}O)_2]$ core with additional multidentate ligands.[36−39] The short internuclear Mo−Mo distance of 2.5432(5) Å is indicative of an Mo−Mo single bond, consistent with the observed diamagnetism of the complex.

The bromide ion (not depicted in Figure 3) is involved in hydrogen bond interactions with the two NH groups, with Br···N contacts of 3.258(4) Å and 3.358(4) Å [Br···N(5) and Br···N(2), respectively]. Two very similar crystal structures

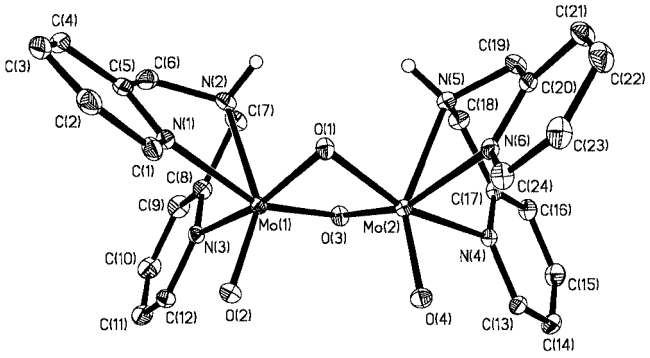

Figure 3. ORTEP representation for the cationic part in **4** with thermal ellipsoids at 50% probability level; hydrogen atoms, except amine hydrogen atoms, have been omitted for clarity

Table 2. Selected bond lengths [Å] and bond angles [°] for [Mo_2-$(bpa)_2(O)_2(\mu\text{-}O)_2$](Br,$PF_6$) (**4**)

Mo(1)−N(1)	2.219(2)	Mo(2)−N(6)	2.227(2)
Mo(1)−N(2)	2.313(2)	Mo(2)−N(5)	2.294(2)
Mo(1)−N(3)	2.263(2)	Mo(2)−N(4)	2.245(2)
Mo(1)−O(2)	1.687(2)	Mo(2)−O(4)	1.692(2)
Mo(1)−O(1)	1.934(2)	Mo(2)−O(1)	1.921(2)
Mo(1)−O(3)	1.935(2)	Mo(2)−O(3)	1.933(2)
Mo(1)−Mo(2)	2.5432(5)		
O(1)−Mo(1)−O(2)	110.10(7)	O(1)−Mo(2)−O(4)	110.70(7)
O(3)−Mo(1)−O(2)	111.83(7)	O(3)−Mo(2)−O(4)	112.29(7)
O(1)−Mo(1)−O(3)	91.43(6)	O(1)−Mo(2)−O(3)	91.88(6)
Mo(1)−O(1)−Mo(2)	82.55(6)	Mo(2)−O(3)−Mo(1)	82.22(6)

with ethyl or methylethyl linkers between the two bpa ligands have been reported,[37] and these display Mo-donor atom bond lengths nearly identical to those in **4**. Apparently, the hydrogen-bonded bromide ion forces the bpa ligands into the same conformation as the ethyl and methylethyl linkers do. It would be expected that this bromide ion would be bound very tightly because, apart from hydrogen bond interactions, it is also involved in an electrostatic interaction with the dinuclear molybdenum complex of charge 2+.

NMR Spectroscopy

In solution, the hydrogen atoms of the picolyl-CH_2 groups become magnetically inequivalent due to metal coordination of the three nitrogen atoms. Therefore, the ^1H NMR spectrum of **2** showed two doublets at $\delta = 4.67$ and $\delta = 3.72$ with intensity two and a ^2J coupling constant of 15.5 Hz (see Supporting Information, Figure S1). In the ^1H NMR spectrum of **1** on the other hand, the appearance of the picolyl-CH_2 hydrogen atom resonances was influenced by the amine NH group. This NH hydrogen atom resonated at $\delta = 6.14$, with a ^3J coupling constant of 6.6 Hz. One of the pairs of magnetically inequivalent picolyl-CH_2 hydrogen atoms resonated as a doublet at $\delta = 4.06$, with a ^2J coupling constant of 16.8 Hz, whereas the other pair appeared as a doublet of doublets at $\delta = 4.33$, with a ^2J coupling constant of 16.8 Hz and a ^3J coupling constant of 6.6 Hz. The size of these coupling constants in the ^1H NMR spectrum of **1** can be explained by the Karplus equation.[40] Analysis of the crystallographic data[41] shows that the absolute value of the HNCH torsion angles is close to 30° for one set of protons and close to 90° for the other (see Supporting Information, Figure S2 and Table S3). The calculated $^3J_{H,H}$ values of 5.9 Hz and 0.2 Hz, respectively, are in good agreement with the observed coupling constants in the ^1H NMR spectrum, indicating that the solid-state structure does not differ to any large extent from the structure of **1** in solution.

The ^{13}C NMR spectra of **1** and **2** each showed two signals corresponding to the CO ligands at $\delta \approx 230$ (see Exp. Sect.), with the signal at the higher chemical shift having approximately twice the intensity of the signal at lower frequency. The CO ligand *trans* to the amine nitrogen atom was more shielded due to increased π-backbonding, whereas the CO ligands in positions *trans* to the pyridine groups had to compete with the pyridine rings for π-backbonding.

Results from ^{95}Mo NMR measurements are summarized in Table 3, together with the chemical shifts for several other *fac*-$Mo(CO)_3$ compounds with N-donor ligands, for comparison. The chemical shifts of *fac*-[$Mo(N_3)(CO)_3$] complexes span a range of about 350 ppm, with compounds **1** and **2** showing resonances in the high frequency region of that range. The molybdenum nucleus in **2** was deshielded by 89 ppm compared to complex **1**. This downfield shift upon alkylation of the bis(picolyl)amine nitrogen atom is the reverse of the trend observed for the 1,4,7-triazacyclononane derivatives: [$Mo(Me_3[9]aneN_3)(CO)_3$] resonated 226 ppm upfield from [$Mo([9]aneN_3)(CO)_3$]. At first sight, an upfield shift should be expected, as the electron density at the Mo nucleus increases upon alkylation of the amine ligand. While this is true for the triazacyclononane series, the opposite trend holds for **1** and **2**. However, for heavier elements such as Mo, steric effects such as ligand bulkiness and chelate ring size, as well as local symmetry effects, have an important influence on the chemical shift of the element.[42,43] The downfield shift of **2** with respect to **1** may therefore be explained on the basis of steric effects. In fact, the Mo-donor atom bond lengths in the X-ray crystal struc-

Table 3. ^{95}Mo NMR spectroscopic data of **1**, **2**, and several other *fac*-[$Mo(N_3)(CO)_3$] compounds

Complex	Solvent	δ[a] [ppm]	$\Delta\nu_{1/2}$ [Hz]	Ref.
[$Mo(pyridine)_3(CO)_3$]	Pyridine	−800	7	[44]
[Mo(Bz-bpa)$(CO)_3$] (**2**)	MeCN	−849	47	this work
[$Mo([9]aneN_3)(CO)_3$]	CH_2Cl_2	−866	20	[45]
[Mo(bpa)$(CO)_3$] (**1**)	MeCN	−938	36	this work
[$Mo([12]aneN_3)(CO)_3$]	CH_2Cl_2	−1001	13	[45]
[Mo(dien)$(CO)_3$][b]	$HCONMe_2$	−1088	70	[46]
[$Mo(Me_3[9]aneN_3)(CO)_3$]	DMSO	−1092	160	[45]
[$Mo(MeCN)_3(CO)_3$]	MeCN	−1114	10	[47]
[$Mo\{HB(Me_2pz)_3\}(CO)_3$]$^-$	$HCONMe_2$	−1149	80	[45]

[a] Chemical shifts reported versus 2 M Na_2MoO_4 in D_2O at an apparent pH = 11. [b] dien = diethylenetriamine.

ture of **1** show a trend towards being somewhat shorter than their counterparts in **2**.

Electrochemistry

Both **1** and **2** underwent reversible one-electron oxidations in CH_3CN and CH_2Cl_2 with Bu_4NPF_6 as supporting electrolyte at potentials slightly more negative than the Fc/Fc^+ couple. The redox potentials for these complexes are listed in Table 4, together with those for the related 1,4,7-triazacyclonane (tacn) and hydridotris(3,5-dimethylpyrazolyl)borate [$HB(Me_2pz)_3$] complexes. The redox potentials for **1** and **2** appear to be solvent-dependent, with the lower oxidation potential measured in CH_2Cl_2. Table 4 shows that the oxidation potentials of **1** and **2** are very similar to those of the tacn and Me_3-tacn complexes. The hydridotris(3,5-dimethylpyrazolyl)borate anionic analogue $[Mo\{HB(Me_2pz)_3\}(CO)_3]^-$ undergoes a one-electron oxidation at slightly higher potential than the tacn, bpa and Bz-bpa complexes.

Table 4. Reversible one-electron oxidations of *fac*-$Mo(CO)_3$ compounds with tridentate N-donor ligands

Complex	$E_{1/2}$ (MeCN)[a]	$E_{1/2}$ (CH_2Cl_2)[a]
$[Mo(bpa)(CO)_3]$ (**1**)	−0.26[b]	−0.33[b]
$[Mo(Bz\text{-}bpa)(CO)_3]$ (**2**)	−0.22[b]	−0.28[b]
$[Mo([9]aneN_3)(CO)_3]$	−0.37[b]	−0.34[b]
$[Mo(Me_3[9]aneN_3)(CO)_3]$	−0.25[c]	−0.28[b]
$[Mo\{HB(Me_2pz)_3\}(CO)_3]^-$	0.08[d][e]	0.00[d][e]

[a] 0.1 M Bu_4NPF_6 as supporting electrolyte; vs. Fc/Fc^+; in Volt. [b] This work. [c] From ref.[48] [d] 0.1 M Bu_4NBF_4 as supporting electrolyte. [e] From ref.[49]

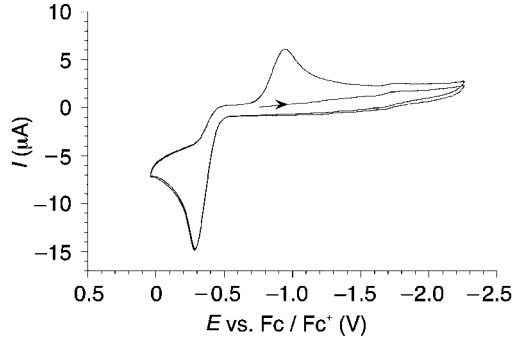

Figure 4. Cyclic voltammogram of **2** (10^{-3} M) in CH_2Cl_2 in the presence of Bu_4NBr (0.1 M); two consecutive cycles (scan rate 200 mV/s) starting from −0.8 V moving first to −2.3 V; note that the reduction peak at −0.95 V appears only in the second cycle

In CH_2Cl_2 and with Bu_4NBr as the supporting electrolyte, the electrochemical behaviour of **1** and **2** was completely different. Irreversible oxidations took place, with peak potentials of −0.37 V vs. Fc/Fc^+ (for **1**) and −0.28 V vs. Fc/Fc^+ (for **2**). Controlled potential coulometry on both compounds established these oxidations as two-electron processes, attributable to formation of the seven-coordinated complexes $[Mo(bpa)(CO)_3Br]^+$ and $[Mo(Bz\text{-}bpa)(CO)_3Br]^+$. Formation of seven-coordinated Mo^{II} species has also been reported for *fac*-$Mo(CO)_3$ complexes with two different tacn derivatives.[25,48] After generation of the seven-coordinated species $[Mo(bpa)(CO)_3Br]^+$ and $[Mo(Bz\text{-}bpa)(CO)_3Br]^+$, single reduction peaks were observed at more negative potentials, namely at −1.20 V vs. Fc/Fc^+ for $[Mo(bpa)(CO)_3Br]^+$ and −0.95 V vs. Fc/Fc^+ for $[Mo(Bz\text{-}bpa)(CO)_3]^+$, as shown in Figure 4 for complex **2**.

The reductive peaks only appeared during the second of two consecutive cyclic voltammograms. This demonstrates that the seven-coordinated complexes formed upon oxidation of the starting material in the first cycle are reduced at this potential. With the aid of controlled potential coulometry, the number of transferred electrons for this reduction process was shown to be two, again yielding the neutral compounds **1** and **2**. The bpa derivatives differ from the tacn analogues in this respect, because the corresponding reduction peak of the seven-coordinated species for the tacn complexes was not observed in the range from −2.0 V to +2.0 V.[25,48] Additional evidence for the chemical reversibility of the two-electron oxidation of **1** and **2** was also obtained from UV and IR spectroelectrochemical investigations (see below).

Electronic Spectroscopy

The electronic spectra of **1** and **2** in MeCN were very similar, each displaying two intense MLCT bands, with maxima at 327 nm ($\varepsilon = 6.1\cdot10^3$ $M^{-1}\cdot cm^{-1}$) and 416 nm ($\varepsilon = 6.9\cdot10^3$ $M^{-1}\cdot cm^{-1}$) for **1** and at 329 nm ($\varepsilon = 6.3\cdot10^3$ $M^{-1}\cdot cm^{-1}$) and 429 nm ($\varepsilon = 7.0\cdot10^3$ $M^{-1}\cdot cm^{-1}$) for **2**.

UV/Vis spectroelectrochemical investigations could only be performed on **2**, since $\mathbf{1}^+$ and $[Mo(bpa)(CO)_3Br]^+$ (the oxidation products of **1**) were both very reactive in solution and partially reacted further during the time required for coulometry (several minutes), probably to yield oxo species. The changes in the electronic spectrum during the electrochemical oxidation of complex **2** in CH_2Cl_2 were monitored with both Bu_4NPF_6 and Bu_4NBr as supporting electrolyte, as depicted in Figure 5. During oxidation, in the presence both of PF_6 and of bromide anions, the MLCT bands at 429 nm and 329 nm gradually disappeared, as a result of the decreased electron availability at the Mo ion in the Mo^I and Mo^{II} forms. With Bu_4NPF_6 as supporting electrolyte (formation of $\mathbf{2}^+$), a new shoulder appeared at around 350 nm, with a molar extinction coefficient of around $4.8\cdot10^3$ $M^{-1}\cdot cm^{-1}$, while an isosbestic point was present at 320 nm. In the presence of bromide anions [formation of $Mo(Bz\text{-}bpa)(CO)_3Br^+$], a new shoulder appeared at 370 nm, with a molar extinction coefficient of around $1.4\cdot10^3$ $M^{-1}\cdot cm^{-1}$, and an isosbestic point was present at 307 nm. After both oxidations, the formed complexes could be reduced at appropriate potentials, once again yielding the UV/Vis spectrum of **2**, without any significant loss in absorbance (i.e., within 99%). This finding is additional evidence for the chemical reversibility of the oxidations.

Infrared Spectroscopy

The infrared spectra of **1** and **2** in THF showed three ν_{CO} vibrations: at 1904, 1790, and 1779 cm^{-1} for **1**, and at 1906,

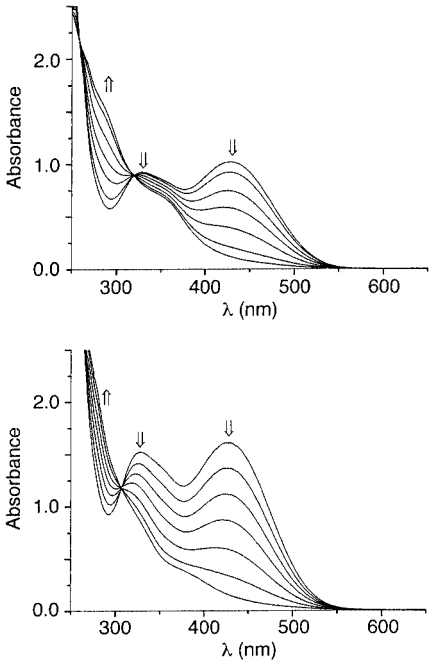

Figure 5. Changes in the electronic spectrum of **2** during coulometry in CH_2Cl_2 at 0° C; top: in the presence of 0.1 M Bu_4NPF_6, one-electron oxidation (formation of $\mathbf{2}^+$), $2.92\cdot10^{-4}$ M of **2**, path-length 0.5 cm; bottom: in the presence of 0.1 M Bu_4NBr, two-electron oxidation {formation of [Mo(Bz-bpa)$(CO)_3$Br]$^+$}, $4.61\cdot10^{-4}$ M of **2**, path length: 0.5 cm

1794, and 1782 cm^{-1} for **2**. This is consistent with C_s symmetry, for which three ν_{CO} vibrations are expected (A′ + 2 A′′). In the case of [Mo(Me_3[9]aneN_3)$(CO)_3$] the three nitrogen atoms are identical, resulting in a complex with C_{3v} symmetry, for which only two infrared-active vibrations should be expected (A_1 + E, at 1907 cm^{-1} and 1773 cm^{-1}, respectively).

The infrared spectrum of [Mo(bpa)(CO)Br]Br_3 (**3**) was measured conventionally between NaCl windows in THF solution, whereas infrared spectra of $\mathbf{1}^+$, $\mathbf{2}^+$, and [Mo(Bz-bpa)$(CO)_3$Br]$^+$ were recorded in situ during electrochemical oxidation of **1** and **2** in an OTTLE cell. As a representative example, the infrared spectral changes during the oxidation of **2** to $\mathbf{2}^+$ are depicted in Figure 6.

The carbonyl stretching vibrations in the infrared spectra of the compounds in this study are summarized in Table 5, together with values of analogous tacn and hydridotris(pyrazolyl)borate compounds. As can be observed, the ν_{CO} stretching vibrations of **1** and **2**, their 17-electron derivatives

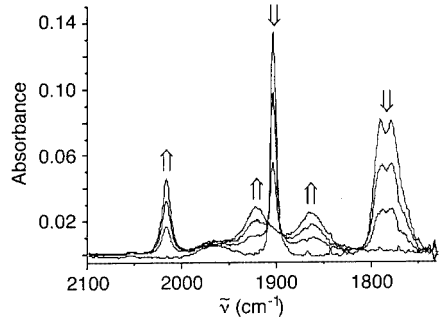

Figure 6. Infrared spectroscopic changes monitored during the one-electron oxidation of **2** to $\mathbf{2}^+$ (1.0 mM) in THF (0.1 M Bu_4NPF_6), performed in an OTTLE cell at 0° C

Table 5. Selected vibrational data for **1**, **2**, **8a**, **8b**, $\mathbf{1}^+$, $\mathbf{2}^+$, **3**, [Mo(Bz-bpa)$(CO)_3$Br]$^+$, and related compounds

Complex	Solvent	ν(CO) [cm^{-1}]	Ref.
Mo^0 compounds:			
[Mo(bpa)$(CO)_3$] (**1**)	THF	1904, 1790, 1779[a]	this work
[Mo(Bz-bpa)$(CO)_3$] (**2**)	THF	1906, 1794, 1782[a]	this work
[Mo(bpa-Phe-OMe)$(CO)_3$] (**8a**)	THF	1906, 1793, 1782[a]	this work
[Mo(bpa-Ala-Phe-OMe)$(CO)_3$] (**8b**)	THF	1906, 1793, 1782[a]	this work
[Mo([9]aneN_3)$(CO)_3$]	THF	1901, 1766[b]	this work
[Mo(Me_3[9]aneN_3)$(CO)_3$]	THF	1907, 1773[b]	this work
[Mo(benzyl$_3$[9]aneN_3)$(CO)_3$]	CH_2Cl_2	1907, 1768[b]	[50]
[Mo{HB(pz)$_3$}$(CO)_3$]$^-$	CH_3CN	1897, 1761[b]	[51]
[Mo{HB(Me_2pz)$_3$}$(CO)_3$]$^-$	CH_3CN	1891, 1751[b]	[51]
[Mo{HB(Me_2pz)$_3$}$(CO)_3$]$^-$	CH_2Cl_2	1884, 1742[b]	[33]
Mo^I compounds:			
[Mo(bpa)$(CO)_3$]$^+$ ($\mathbf{1}^+$)	THF	2015, 1910, 1859[c]	this work
[Mo(Bz-bpa)$(CO)_3$]$^+$ ($\mathbf{2}^+$)	THF	2018, 1922, 1864[c]	this work
[Mo(benzyl$_3$[9]aneN_3)$(CO)_3$]$^+$	CH_2Cl_2	2017, 1909, 1873	[50]
[Mo{HB(pz)$_3$}$(CO)_3$]	CH_2Cl_2	2010, 1885 (br)	[52]
[Mo{HB(Me_2pz)$_3$}$(CO)_3$]	CH_2Cl_2	1998, 1864 (br)	[53]
[Mo{HB(Me_2pz)$_3$}$(CO)_3$]	CH_2Cl_2	2001, 1860 (br)	[33]
Mo^{II} compounds:			
[Mo(bpa)$(CO)_3$Br]$^-$	THF	2055, 1989, 1935	this work
[Mo(Bz-bpa)$(CO)_3$Br]$^-$	CH_3CN	2055, 1980, 1957[c]	this work
[Mo([9]aneN_3)$(CO)_3$Br]$^-$	THF	2042, 1964, 1928	this work
[Mo{HB(pz)$_3$}$(CO)_3$Br]	CH_2Cl_2	2053, 1980, 1938	[54]

[a] Complex has C_s symmetry. [b] Complex has C_{3v} symmetry. [c] Complex generated electrochemically in an OTTLE cell.

$\mathbf{1}^+$ and $\mathbf{2}^+$, and the seven-coordinated complexes **3** and $[Mo(Bz\text{-}bpa)(CO)_3Br]^+$ showed trends similar to those seen with their tacn and hydridotris(pyrazolyl)borate analogues. The electron availability of the molybdenum ion in these species decreases upon increase of the metal ion's oxidation state, resulting in a shift of the ν_{CO} vibrations to higher wavenumbers.

EPR Spectroscopy

Because the electrochemical and spectro-electrochemical investigations on **2** indicated good stability of the one-electron oxidized complex $\mathbf{2}^+$, this latter compound was subjected to EPR spectroscopic investigation. The X-Band EPR spectrum of $\mathbf{2}^+$ (generated by coulometry) as a frozen CH_2Cl_2 solution is depicted in Figure 7, together with the resulting spectrum from the simulation procedure.

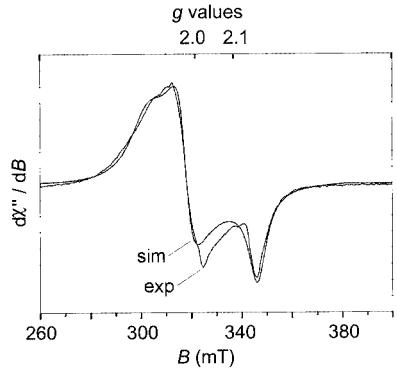

Figure 7. X-Band EPR spectrum of $\mathbf{2}^+$, generated by coulometry, in frozen CH_2Cl_2 solution (0.1 M Bu_4NPF_6) and its simulated spectrum; $T = 50$ K; power: 0.2 mW; frequency: 9.46494 GHz; modulation: 1.25 mT

Although the fit is not perfect, it clearly shows the rhombic nature of the $S = 1/2$ spectrum, with simulated g values $g_x = 2.238$, $g_y = 2.131$, and $g_z = 1.954$. These g values are slightly higher than those reported for $[Mo(benzyl_3[9]aneN_3)(CO)_3]^+$ in a frozen DMF solution, which were $g_x = 2.188$, $g_y = 2.040$, and $g_z = 1.992$.[50] The discrepancy between the simulated and the experimental spectrum of $\mathbf{2}^+$ might be due to the presence of small amounts of paramagnetic decomposition products. Indeed, no satisfactory EPR spectra of the related compound $\mathbf{1}^+$ could be obtained, because the EPR spectra contained several additional resonances. As mentioned above, the spectro-electrochemical investigations on **1** showed that $\mathbf{1}^+$ had partially decomposed during the time required for the coulometry (several minutes).

Labelling of Biomolecules

Complex **2** showed particularly good stability towards dioxygen and water. We have therefore set out to use this type of $(bpa)Mo(CO)_3$ derivative for the labelling of biomolecules, in particular amino acids and peptides. The synthetic strategy is outlined in Scheme 3. The ligand *N*-(*p*-carboxybenzyl)bis(2-picolyl)amine (**6**) was prepared in good yield from methyl *p*-(bromomethyl)benzoate and bis(2-picolyl)amine, followed by base hydrolysis of the methyl ester. With TBTU [*O*-(1*H*-benzotriazol-1-yl)-*N*,*N*,*N*′,*N*′-tetramethyluronium tetrafluoroborate] as the activating reagent, **6** was coupled to the amino groups of phenylalanine methyl ester and the dipeptide alanyl-phenylalanine methyl ester to yield **7a** and **7b**, respectively. With a view to future applications in the labelling of more sensitive biomolecules, **7** was not treated directly with $Mo(CO)_6$, because of the vigorous conditions required for quantitative labelling. Instead, the *fac*-$Mo(CO)_3$ fragment was introduced under very mild conditions, by treatment with $[Mo(CO)_3(EtCN)_3]$. After 5−10 min of stirring at room temperature, an orange precipitate formed. After filtration and drying in vacuo, compounds **8a** and **8b** were obtained in pure form in 80% yield.

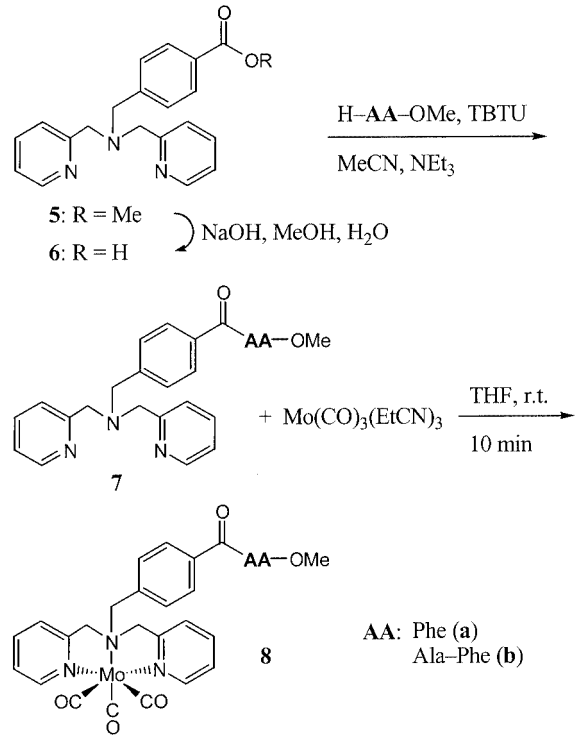

Scheme 3

The spectroscopic data of **8a** and **8b** confirmed the proposed constitution of the bioconjugates. First of all, the IR spectra showed three ν_{CO} vibrations at 1906, 1793, and 1782 cm^{-1} (Table 5). A ^{95}Mo NMR resonance was observed at $\delta = -849$ for both compounds, identical to the chemical shift of **2**. In addition, resonances for the metal carbonyl ligands at $\delta \approx 230$ were observed in the ^{13}C NMR spectra. Coordination of the *fac*-$Mo(CO)_3$ fragment to the nitrogen atoms of the substituted bpa ligand was also evident in the ^1H NMR spectra. The hydrogen atoms of the picolyl-CH_2 groups are magnetically inequivalent, forming an AB system with a coupling constant of about 15.5 Hz. Unlike in **2**, an additional small coupling of 1.5 Hz (**8a**) and 3.4 Hz (**8b**) was observed. All other NMR signals could be as-

signed unambiguously by analogy with **2** and with the help of 2D NMR spectroscopy. Finally, both compounds **8a** and **8b** were reversibly oxidized at −0.27 V vs. Fc/Fc^+ in CH_2Cl_2. All of these analytical properties demonstrated that neither the carbonyl group nor the attached biomolecule have a strong influence on the spectroscopic properties of the Mo(bpa)$(CO)_3$ group.

Discussion

The experimental and spectroscopic results described above show that the properties of **1** and **2** are similar to those of their 1,4,7-triazacyclonane and hydridotris(pyrazolyl)borate analogues. However, differences in reactivity and electrochemical behaviour between these three types of compounds were observed. Compounds **1** and **2** showed reversible one-electron oxidations with Bu_4NPF_6 as supporting electrolyte at potentials similar to those for the tacn derivatives, whereas the Mo^0/Mo^I transition for [Mo{HB$(Me_2pz)_3$}$(CO)_3]^-$ occurred at a slightly higher potential. With Bu_4NBr as supporting electrolyte, **1** and **2** each underwent electrochemically irreversible two-electron oxidation, to yield the seven-coordinated complexes [Mo(bpa)$(CO)_3Br]^+$ and [Mo(Bz-bpa)$(CO)_3Br]^+$, respectively. These Mo^{II} complexes could be reduced once more at a potential of around −1.0 V, again yielding complexes **1** and **2**. For the complexes [Mo(R_3-tacn)$(CO)_3$] (R = Me or benzyl), electrochemical formation of [Mo(R_3-tacn)$(CO)_3Br]^+$ was reported, but the corresponding re-reduction to yield the Mo^0 complexes was not observed between +2.0 V and −2.0 V.[25,48] One difference in reactivity between [Mo(bpa)$(CO)_3Br]^+$ and [Mo(tacn)$(CO)_3Br]^+$ is that the latter compound could be crystallized from aerobic aqueous solutions,[35] whereas the former reacted further to yield the dinuclear Mo^V complex [Mo_2(bpa)$_2(O)_2$(μ-$O)_2$](Br,PF_6).

Another difference from the analogous tacn and hydridotris(pyrazolyl)borate complexes was observed in the solution infrared spectra of **1** and **2**, since **1** and **2** have point-group symmetry C_s, whereas the tacn and hydridotris(pyrazolyl)borate complexes are of point-group symmetry C_{3v}. The degeneracy of the vibrations of *E* symmetry in the tacn and hydridotripyrazolylborate complexes is abolished in **1** and **2**.

A suitable organometallic labelling group for biomolecules must be readily introducible. For both the tacn and pyrazolylborate ligands, selective monosubstitution with a handle for labelling is difficult to achieve. The bpa ligand, on the other hand, is readily substituted with a carboxylic acid group. Reaction between (activated) organometallic acids and free amino groups in the biomolecule has long been known to be a successful strategy.[55−60] Secondly, the bioconjugate must be stable in water and air for quite some time. In addition, the property of the labelling group that is to be used for detection of the conjugate should not depend much on the attached biomolecule. Jaouen and coworkers have developed IR spectroscopy of bioorganometallic compounds into an immunoassay (*C*arbonyl *M*etallo *I*mmuno *A*ssay, CMIA) and thereby demonstrated the suitability of IR spectroscopy as a sensitive and reliable detection method.[2,4,61,62] We have recently reported amino acid and peptide derivatives of [CpMo(allyl)$(CO)_2$].[7] These compounds were readily isolated in the presence of water and showed promising spectroscopic properties. However, they could not be reversibly oxidized and did not show the required long-term stability in air. We were then able to show that isolobal replacement of the cyclopentadienyl ligand with histidinate resulted in complexes of the general type [Mo(His)(allyl)$(CO)_2$], with very favourable electrochemical properties and much increased stability towards air even in solution.[8,9]

In this work, we have demonstrated that *fac*-Mo$(CO)_3$ derivatives of the bpa ligand are well suited for the labelling of biomolecules. On comparing benzyl-substituted [Mo(Bz-bpa)$(CO)_3$] (**2**) to the bioconjugates **8** we note that there is very little influence of the attached biomolecule on the spectroscopic properties of the metal complex. Owing to this property, as well as its demonstrated stability in an aqueous, aerobic environment, this group is a well-suited marker for biomolecules. We are currently extending the chemistry described here to other biomolecules, as well as towards solid-phase synthesis of peptides.

Experimental Section

General: All syntheses and manipulations of the metal complexes were performed under argon by standard Schlenk techniques, unless otherwise noted. All solvents were deoxygenated before use unless otherwise noted. Elemental analyses were performed by H. Kolbe, Microanalytisches Laboratorium, Mülheim/Ruhr, Germany. Infrared spectra were recorded with a Perkin−Elmer FT-IR spectrophotometer 2000 as KBr disks and/or in THF solutions between NaCl windows (either a 0.5-mm or 1.0-mm spacer), with a spectral resolution of either 2.0 cm^{-1} or 4.0 cm^{-1}. For the IR spectroelectrochemical measurements, an OTTLE cell consisting of CaF_2 windows with a pathlength of 0.17 mm was used (2.0 cm^{-1} resolution). ^1H and ^{13}C NMR spectra were recorded with Bruker ARX 250 (^1H at 250.13 MHz), Bruker DRX 400 (^1H at 400.13 MHz) and Bruker DRX 500 (^1H at 500.35 MHz) spectrometers. The spectra were referenced to TMS, using the ^{13}C or residual protio signals of the deuterated solvents as internal standards. ^{95}Mo NMR spectra were recorded with a Bruker DRX 500 spectrometer (32.6 MHz for ^{95}Mo), with a 2 M Na_2MoO_4 solution in D_2O at an apparent pH = 11 as an external standard. Mass spectra in the electron impact mode (EI; 70 eV) were recorded with a Finnigan MAT 8200 mass spectrometer. Only characteristic fragments are given, with intensities in parentheses and possible composition between brackets. The spectra were normalized against the most intense peak, which therefore had intensity 100%. ElectroSpray Ionisation mass spectra (ESI-MS) in the positive ion mode were recorded with a Hewlett−Packard HP 5989 mass spectrometer. The solvent used is given in parentheses, and the possible composition of the peaks is between brackets. Electronic spectra were recorded with a Hewlett−Packard HP 8452A diode array spectrophotometer. Cyclic voltammograms and square-wave voltammograms in CH_2Cl_2 or MeCN solutions with Bu_4NPF_6 or Bu_4NBr as supporting electrolytes were recorded with an EG&G Potentiostat/Galvanostat 273A.

A three-electrode cell was employed, with a glassy-carbon working electrode, a platinum-wire auxiliary electrode and an $Ag/AgNO_3$ reference electrode (0.01 M $AgNO_3$ in MeCN). For determination of the redox potentials, ferrocene was added as an internal standard. Controlled potential coulometry measurements (both for preparative purposes and for UV/Vis spectroelectrochemical studies) were performed in CH_2Cl_2 solutions with the same supporting electrolytes by employing the potentiostat described above, but with a Pt-grid as working electrode, a Pt-brush auxiliary electrode separated from the working electrode compartment by a vycor frit and a $Ag/AgNO_3$ (0.01 M $AgNO_3$ in MeCN) reference electrode. Thin layer infrared spectro-electrochemical measurements were performed with an OTTLE cell of 0.17 mm optical pathlength consisting of a Pt-grid working electrode, a glassy-carbon counterelectrode and a Ag-wire as "quasi-reference electrode". The EPR spectrum was recorded as a frozen solution (generated by controlled potential coulometry) with a Bruker ESP 300E spectrometer, equipped with an ER 041 XK-D microwave bridge. The EPR spectrum was simulated with the program GFIT.[63] Bis(2-picolylamine) and $Mo(CO)_6$ were purchased from Aldrich. The compounds *N*-benzylbis(2-picolyl)amine,[64] $[Mo([9]aneN_3)(CO)_3]$,[35] $[Mo([9]aneN_3(CO)_3Br]Br_3$,[35] $[Mo(Me_3[9]aneN_3)(CO)_3]$,[48] and $[Mo(CO)_3(EtCN)_3]$[65] were synthesized according to literature procedures.

Compound 1: A suspension of bis(2-picolyl)amine (1.0 g, 5.0 mmol) and $Mo(CO)_6$ (1.3 g, 5.0 mmol) in degassed di-*n*-butyl ether (75 mL) was heated at 150 °C for 1 h, during which a deep yellow precipitate formed. After the mixture had been allowed to reach room temperature, the solid material was collected by filtration and dried in vacuo. Yield: 1.8 g (95%). Crystals suitable for X-ray analysis were grown by slow concentration of a CH_3CN/H_2O mixture (5:1, v/v) under a stream of argon. $C_{15}H_{13}MoN_3O_3$ (379.22): calcd. C 47.51, H 3.46, N 11.08; found C 47.15, H 3.40, N 11.03. IR (KBr): $\tilde{\nu}$ = 3323 (w) ν_{NH}, 1901 (s), 1891 (vs), 1784 (s), 1769 (s), 1742 (vs) ν_{CO}. IR (THF): $\tilde{\nu}$ = 1904 (vs), 1790 (s), 1779 (s) ν_{CO}. MS (EI): *m/z* (%) = 381 (14) $[M^+]$, 353 (2) $[M - CO]^+$, 325 (1) $[M - 2\,CO]^+$, 297 (31) $[M - 3\,CO]^+$, 93 (100). ^1H NMR ($[D_6]$DMSO, 400.13 MHz): δ = 8.73 (app. d, 2 H, H_{Pyr}), 7.65 (m, 2 H, H_{Pyr}), 7.27 (app. d, 2 H, H_{Pyr}), 7.14 (pseudo t, 2 H, H_{Pyr}), 6.14 (t, $^3J_{H,H}$ = 6.6 Hz, 1 H, NH), 4.33 (dd, $^2J_{H,H}$ = 16.8, $^3J_{H,H}$ = 6.6 Hz, 2 H, CH_2), 4.06 (d, $^2J_{H,H}$ = 16.8 Hz, 2 H, CH_2). ^{13}C NMR ($[D_6]$DMSO, 62.9 MHz): δ = 231.4, 229.3 (CO), 159.5, 150.1, 137.5, 123.0, 122.0 (C_{Pyr}), 59.6 (CH_2). ^{95}Mo NMR (CH_3CN, 32.6 MHz): δ = −938 ($\Delta_{1/2}$ = 36 Hz).

Compound 2: A suspension of *N*-benzylbis(2-picolyl)amine (0.96 g, 3.30 mmol) and $Mo(CO)_6$ (0.88 g, 3.30 mmol) in deoxygenated mesitylene (40 mL) was heated at 150° C for 1 h, during which an orange solid precipitated. After the mixture had been allowed to cool to ambient temperature, the precipitate was isolated by filtration, washed with *n*-hexane (10 mL) and dried in vacuo. Yield: 1.28 g (83%). Crystals suitable for X-ray structure determination were grown by slow concentration of a CH_3CN/H_2O (10:1, v/v) solution under a stream of argon. $C_{22}H_{19}MoN_3O_3$ (469.34): calcd. C 56.30, H 4.08, N 8.95; found C 56.18, H 4.02, N 9.05. IR (KBr): $\tilde{\nu}$ = 1898 (vs), 1776 (s), 1752 (vs) ν_{CO}. IR (THF): $\tilde{\nu}$ = 1906 (vs), 1794 (s), 1782 (s) ν_{CO}. MS (EI): *m/z* (%) = 471 (6) $[M^+]$, 443 (4) $[M - CO]^+$, 387 (13) $[M - 3\,CO]^+$, 197 (100). ^1H NMR ($[D_6]$DMSO, 400.13 MHz): δ = 8.68 (app. d, 2 H, H_{Pyr}), 7.68 (m, 2 H, H_{Ar}), 7.59 (m, 2 H, H_{Ar}), 7.46 (m, 3 H, H_{Ar}), 7.16 (pseudo d, 2 H, H_{Ar}), 7.08 (m, 2 H, H_{Ar}), 4.67 (d, $^2J_{H,H}$ = 15.5 Hz, 2 H, CH_2), 4.66 (s, 2 H, $CH_{2,Bz}$), 3.72 (d, $^2J_{H,H}$ = 15.5 Hz, 2 H, CH_2). ^{13}C NMR (CD_3CN, 125.8 MHz): δ = 232.3, 231.3 (CO), 159.9, 151.6, 138.4, 133.6, 132.5, 129.7, 129.4, 124.1, 123.3 (C_{Ar}), 71.0 ($CH_{2,Bz}$), 65.4 (CH_2). ^{95}Mo (CH_3CN, 32.6 MHz): δ = −849 ($\Delta_{1/2}$ = 47 Hz).

Compound 3: Br_2 (1.0 g, 0.3 mL, 6.3 mmol) was added dropwise to a suspension of **1** (0.5 g, 1.3 mmol) in degassed $CHCl_3$ (50 mL), resulting in a clear orange-red solution. The mixture was stirred for 45 min, during which an orange-brown powder precipitated. The solid was collected by filtration, washed with $CHCl_3$ (10 mL) and pentane (10 mL) and air-dried. Yield: 0.66 g (73%). $C_{15}H_{13}Br_4MoN_3O_3$ (698.84): calcd. C 25.78, H 1.88, N 6.01; found C 25.20, H 1.79, N 5.97. IR (KBr): $\tilde{\nu}$ = 3155 (w) ν_{NH}, 2037 (s), 1950 (br, vs) ν_{CO}. IR (THF): $\tilde{\nu}$ = 2055 (s), 1989 (s), 1935 (s) ν_{CO}. MS (ESI-pos., CH_2Cl_2): *m/z* = 460 $[Mo(bpa)(CO)_3Br]^+$, 432 $[Mo(bpa)(CO)_2Br]^+$, 404 $[Mo(bpa)(CO)Br]^+$, 376 $[Mo(bpa)Br]^+$.

Compound 4: $[Mo(bpa)(CO)_3Br]Br_3$ (**3**, 0.5 g, 0.7 mmol) was dissolved in MeOH (30 mL) under aerobic conditions, followed by addition of a KPF_6 (0.66 g, 3.60 mmol) solution in H_2O (10 mL). Upon standing overnight, an orange powder formed; this was isolated by filtration, washed with Et_2O (15 mL) and air-dried. Yield: 0.21 g (68%). Crystals suitable for X-ray diffraction were obtained by slow concentration of an MeOH solution. $C_{24}H_{26}BrF_6Mo_2N_6O_4P$ (879.25): calcd. C 32.78, H 2.98, N 9.56; found 32.67, H 2.91, N 9.47. IR (KBr): $\tilde{\nu}$ = 962 (m) $\nu_{Mo=O}$, 747 (m) $\nu_{as}[M - O]$. MS (ESI-pos., MeOH): *m/z* = 737 $[M - PF_6]^+$, 657 $[M - PF_6 - HBr]^+$, 327 $[M - PF_6 - Br]^{2+}$. ^{13}C NMR ($[D_6]$DMSO, 62.9 MHz): δ = 158.6, 151.7, 142.4, 125.7, 124.2 (C_{Pyr}), 55.3 (CH_2). ^1H NMR ($[D_6]$DMSO, 250.13 MHz) shows broadened signals at room temperature. This could be due to paramagnetic impurities or coalescence as found for a related compound.[37]

Compound 5: NEt_3 (0.69 mL, 5.00 mmol) was added to a solution of bis(2-picolyl)amine (1.0 g, 5.0 mmol) and methyl *p*-(bromomethyl)benzoate (1.15 g, 5.00 mmol) in THF (35 mL), and the mixture was refluxed for 1.5 h. The mixture was allowed to reach room temperature and subsequently filtered to remove a white precipitate. After removal of the solvent under reduced pressure, the oily residue was redissolved in Et_2O (40 mL) and filtered to remove a red solid. Evaporation of the solvent yielded 1.4 g (81%) of a light orange oil, which was used as such in the next step. $C_{21}H_{21}N_3O_2$ (347.4). MS (EI): *m/z* = 347 (2) $[M^+]$, 316 (2) $[M - OCH_3]^+$, 255 (100) $[M - C_6H_6N]^+$. ^1H NMR ($CDCl_3$, 250.1 MHz): δ = 8.49 (app. d, 2 H, H_{pyr}), 7.95 (d, $^3J_{H,H}$ = 8.3 Hz, 2 H, H_{Ar}), 7.62 (pseudo t, 2 H, H_{pyr}), 7.52 (pseudo d, 2 H, H_{pyr}), 7.46 (d, ^3J = 8.3 Hz, 2 H, H_{Ar}), 7.12 (pseudo t, 2 H, H_{pyr}), 3.87 (s, 3 H, OCH_3), 3.78 (s, 4 H, $CH_{2,picolyl}$), 3.71 (s, 2 H, CH_2). ^{13}C ($CDCl_3$, 100.6 MHz): δ = 166.9 (C=O), 159.3 (C_q, pyr), 148.9 (C_{Pyr}), 144.5 ($C_{Ar,q}$), 136.3 (C_{Pyr}), 129.5 (C_{Ar}), 128.9 ($C_{Ar,q}$), 128.6 (C_{Ar}), 122.7 (C_{Pyr}), 122.0 (C_{Pyr}), 60.0 (CH_2, picolyl), 58.1 (CH_2), 51.9 (OCH_3).

Compound 6: A solution of NaOH (0.8 g, 20 mmol) in 5 mL of H_2O was added to a solution of **5** (1.4 g, 4.0 mmol) in MeOH (20 mL), and the mixture was stirred for 2 h at ambient temperature. The pH was adjusted to 7 by dropwise addition of 2 M HCl, followed by removal of the solvent under reduced pressure. The sticky white residue was triturated with $CHCl_3$ (200 mL), followed by filtration to remove NaCl. The $CHCl_3$ solution was dried with $MgSO_4$. Removal of the solvent under reduced pressure afforded a yellow sticky oil, to which CH_3CN (30 mL) was added, followed by vigorous stirring. After approximately 15−30 min, a white precipitate formed. The solution was stored at 0 °C for 2 h, to effect further precipitation and the white solid was then isolated by filtration and dried in vacuo. Yield 0.7 g (53%). $C_{20}H_{19}N_3O_2$ (333.4). IR (KBr): $\tilde{\nu}$ = 1698 (m) $\nu_{C=O}$. MS (EI): *m/z* = 333 (1) $[M]^+$, 241 (100)

$[M - C_6H_6N]^+$. ^1H NMR ($CDCl_3$, 250.1 MHz): δ = 11.35 (br, 1 H, CO_2H), 8.59 (app. d, 2 H, H_{Pyr}), 8.01 (d, $^3J_{H,H}$ = 8.0 Hz, 2 H, H_{Ar}), 7.66 (pseudo t, 2 H, H_{Pyr}), 7.59 (app. d, 2 H, H_{Pyr}), 7.44 (d, $^3J_{H,H}$ = 7.7 Hz, 2 H, H_{Ar}), 7.80 (pseudo t, 2 H, H_{Pyr}), 3.85 (s, 4 H, CH_2), 3.73 (s, 2 H, $CH_{2,Bz}$). ^{13}C NMR ($CDCl_3$, 62.9 MHz): δ = 169.3 (C=O), 159.8, 148.4, 143.1, 137.2, 130.0, 128.8, 123.4, 122.4, 122.0 (all C_{Ar}), 59.3 (CH_2), 58.2 ($CH_{2,Bz}$).

Compound 7a: NEt_3 (1.0 mL, 0.7 g, 7.2 mmol), phenylalanine methyl ester hydrochloride (216 mg, 1.0 mmol), and TBTU (323 mg, 1.0 mmol) were added to a suspension of **6** (333 mg, 1.0 mmol) in CH_3CN (10 mL), and the mixture was stirred for 30 min at ambient temperature. After evaporation of the solvent in vacuo, CH_2Cl_2 (100 mL) was added to the sticky residue, followed by filtration to remove ammonium salts. The CH_2Cl_2 solution was washed with aqueous 2 M $NaHCO_3$ (75 mL) and the phases were separated. The aqueous phase was extracted with CH_2Cl_2 (2 × 75 mL) and the combined organic extracts were dried with $MgSO_4$. Most of the solvent was removed under reduced pressure, followed by further evaporation of the solvent in vacuo, affording a light yellow, glassy solid. Yield: 440 mg (89%). $C_{30}H_{30}N_4O_3$ (494.6). MS (EI): *m*/*z* = 494 (3) $[M]^+$, 463 (1) $[M - OCH_3]^+$, 435 (2) $[M - CO_2CH_3]^+$, 402 (100) $[M - C_6H_6N]^+$. ^1H NMR ($CDCl_3$, 250.13 MHz): δ = 8.49 (m, 2 H, H_{pyr}), 7.63 (m, 4 H, H_{Ar}), 7.50 (d, $^3J_{H,H}$ = 7.9 Hz, 2 H, H_{Ar}), 7.43 (d, $^3J_{H,H}$ = 7.9 Hz, 2 H, H_{Ar}), 7.24 (m, 3 H, H_{Ar}), 7.01 (m, 4 H, H_{Ar}), 6.57 (d, $^3J_{H,H}$ = 8.2 Hz, 1 H), 5.06 (m, 1 H, $C_\alpha H$), 3.76 (s, 4 H, CH_2), 3.72 (s, 3 H, OCH_3), 3.68 (s, 2 H, $CH_{2,Bz}$), 3.21 (m, 2 H, $C_\beta H_2$). ^{13}C NMR ($CDCl_3$, 62.9 MHz): δ = 172.1 ($C{=}O_{ester}$), 166.9 ($C{=}O_{amide}$), 159.0, 148.7, 142.9, 136.7, 136.0, 132.6, 129.1, 128.8, 128.5, 127.1, 127.0, 122.9, 122.2 (C_{Ar}), 59.7 (CH_2), 58.0 ($CH_{2,Bz}$), 53.6, 52.3 (C_α and OCH_3), 37.6 (C_β).

Compound 7b: The dipeptide Boc-Ala-Phe-OMe (350 mg, 1.0 mmol) was dissolved in CH_2Cl_2 (5 mL) and CF_3CO_2H (10 mL), and the mixture was stirred for 1 h at room temperature. After removal of the solvent in vacuo, Et_2O (15 mL) was added to the residue, followed by removal of the solvent in vacuo. This last step was performed three times in order to remove any traces of trifluoroacetic acid. The solid, white residue was suspended in CH_3CN (10 mL), followed by addition of NEt_3 (1.50 mL, 1.09 g, 10.8 mmol), compound **6** (333 mg, 1.0 mmol), and TBTU (323 mg, 1.0 mmol). After the mixture had been stirred at ambient temperature for 30 min, the solvent was removed in vacuo. To the sticky residue was added CH_2Cl_2 (100 mL), followed by filtration to remove ammonium salts. The CH_2Cl_2 solution was washed with aqueous $NaHCO_3$ (2 M, 75 mL), followed by separation of the phases. The aqueous phase was extracted with CH_2Cl_2 (2 × 75 mL), and the combined organic extracts were dried with $MgSO_4$. Most of the CH_2Cl_2 was removed under reduced pressure, followed by further evaporation of the solvent in vacuo, affording a white glassy solid. Yield: 520 mg (92%). $C_{33}H_{35}N_5O_4$ (565.7). MS (EI): *m*/*z* = 565 (6) $[M]^+$, 534 (3) $[M - OCH_3]^+$, 506 (1) $[M - CO_2CH_3]^+$, 473 (100) $[M - C_6H_6N]^+$. ^1H NMR ($CDCl_3$, 400.13 MHz): δ = 8.51 (app. d, 2 H, H_{Pyr}), 7.69 (m, 4 H, H_{Ar}), 7.53 (d, $^3J_{H,H}$ = 7.9 Hz, 2 H, H_{Ar}), 7.46 (d, $^3J_{H,H}$ = 7.9 Hz, 2 H, H_{Ar}), 7.18 (m, 2 H, H_{Ar}), 7.06 (m, 5 H, H_{Ar}), 6.92 (m, 2 H, both NH), 4.80 (m, 1 H, $C_\alpha H$), 4.66 (m, 1 H, $C_\alpha H$), 3.91 (s, 4 H, CH_2), 3.82 (s, 2 H, $CH_{2,Bz}$), 3.67 (s, 3 H, OCH_3), 3.09 (m, 1 H, $C_{\beta,Phe}H$), 3.00 (m, 1 H, $C_{\beta,Phe}H$), 1.40 (d, $^3J_{H,H}$ = 7.0 Hz, 3 H, CH_3). ^{13}C NMR ($CDCl_3$, 100.6 MHz): δ = 172.0, 171.7 ($C{=}O_{ester}$ and $C{=}O_{Ala\text{-}Phe}$), 166.7 (C=O), 157.7, 148.4, 137.3, 135.7, 132.9, 129.2, 129.1, 128.4, 127.3, 127.0, 123.5, 122.6 (C_{Ar}), 59.2 (CH_2), 58.1 ($CH_{2,Bz}$), 53.4, 52.3 (OCH_3 and $C_{\alpha,Phe}$), 49.0 ($C_{\alpha,Ala}$), 37.7 ($C_{\beta,Phe}$), 18.2 ($CH_{3,Ala}$).

Compound 8a: A solution of **7a** (0.40 g, 0.80 mmol) in THF (10 mL) was added dropwise to a stirred solution of $Mo(CO)_3(NCEt)_3$ (0.28 g, 0.80 mmol) in THF (15 mL). The mixture was stirred for 10 min at room temperature, during which an orange precipitate formed. The mixture was concentrated to about 15 mL in vacuo, and the orange solid was collected by filtration, washed with Et_2O (10 mL) and dried in vacuo. Yield: 0.44 g (82%). $C_{33}H_{30}MoN_4O_6$ (674.55): calcd. C 58.76, H 4.48, N 8.31; found C 53.13, H 4.67, N 8.92; (repeated attempts did not improve the C values). IR (KBr): $\tilde{\nu}$ = 1900 (vs) ν_{CO}, 1779 (s) ν_{CO}, 1759 (s) ν_{CO} + $\nu_{C=O}$. IR (THF): $\tilde{\nu}$ = 1906 (vs), 1793 (s), 1782 (s) ν_{CO}. MS (FAB-pos.; dimethoxybenzyl alcohol): *m*/*z* = 676 $[M]^+$, 648 $[M - CO]^+$. ^1H NMR (CD_3CN, 500.35 MHz): δ = 8.77 (m, 2 H, H_{Pyr}), 7.81 (d, $^3J_{H,H}$ = 8.1 Hz, 2 H, H_{Ar}), 7.62 (d, $^3J_{H,H}$ = 8.1 Hz, 2 H, H_{Ar}), 7.49 (m, 2 H, H_{Ar}), 7.31 (m, 5 H, NH and $H_{Ar,Phe}$), 7.24 (m, 1 H, $H_{Ar,Phe}$), 7.00 (m, 4 H, H_{Pyr}), 4.92 (m, 1 H, $C_\alpha H$), 4.76 (s, 2 H, $CH_{2,Bz}$), 4.51 (d, $^2J_{H,H}$ = 15.4 Hz, 2 H, CH_2), 3.73 (dd, $^2J_{H,H}$ = 15.4, $^4J_{H,H}$ = 1.6 Hz, 2 H, CH_2), 3.69 (s, 3 H, OCH_3), 3.32 (m, 1 H, $C_\beta H$), 3.17 (m, 1 H, $C_\beta H$). ^{13}C NMR (CD_3CN, 125.8 MHz): δ = 232.3, 231.3 (CO), 173.1 ($C{=}O_{ester}$), 167.4 ($C{=}O_{amide}$), 159.8, 151.7, 138.4, 138.3, 137.1, 135.0, 132.8, 130.2, 129.5, 128.2, 127.8, 124.1, 123.3 (C_{Ar}), 70.4 ($CH_{2,Bz}$), 65.5 (CH_2), 55.2, 52.9 (OCH_3 + C_α), 38.0 (C_β).

Compound 8b: A solution of **7b** (0.40 g, 0.80 mmol) in THF (10 mL) was added dropwise to a stirred solution of $Mo(CO)_3(NCEt)_3$ (0.28 g, 0.80 mmol) in THF (15 mL). Stirring was continued for 10 min at room temperature, during which an orange precipitate formed. The mixture was concentrated to about 15 mL in vacuo, and the orange solid was collected by filtration, washed with Et_2O (10 mL) and dried in vacuo. Yield: 0.47 g (79%). $C_{36}H_{35}MoN_5O_7$ (745.63): calcd. C 57.99, H 4.73, N 9.39; found C 58.09, H 4.82, N 9.26. IR (KBr): $\tilde{\nu}$ = 1900 (vs) ν_{CO}, 1778 (s) ν_{CO}, 1761 (s) ν_{CO} + $\nu_{C=O}$. IR (THF): $\tilde{\nu}$ = 1906 (vs), 1793 (s), 1782 (s) ν_{CO}. MS (FAB-pos.; dimethoxy benzyl alcohol): *m*/*z* = 747 $[M]^+$, 719 $[M - CO]^+$. ^1H NMR ([D$_6$]DMSO, 500.35 MHz): δ = 8.69 (app. d, 2 H, H_{Pyr}), 8.49 (d, $^3J_{H,H}$ = 7.6 Hz, 1 H, NH), 8.30 (d, $^3J_{H,H}$ = 7.6 Hz, 1 H, NH), 7.97 (d, $^3J_{H,H}$ = 8.1 Hz, 2 H, H_{Ar}), 7.80 (d, $^3J_{H,H}$ = 8.1 Hz, 2 H, H_{Ar}), 7.59 (pseudo t, 2 H, H_{Pyr}), 7.22 (m, 5 H, $H_{Ar,Phe}$), 7.15 (app. d, 2 H, H_{Pyr}), 7.09 (pseudo t, 2 H, H_{Ar}), 4.72 (s, 3 H, $CH_{2,Bz}$ and CH_2), 4.69 (d, $^4J_{H,H}$ = 3.4 Hz, 1 H, CH_2), 3.71 (dd, $^2J_{H,H}$ = 15.7, $^4J_{H,H}$ = 3.4 Hz, 2 H, CH_2), 4.56 (m, 1 H, $C_\alpha H$), 4.50 (m, 1 H, $C_\alpha H$), 3.59 (s, 3 H, OCH_3), 3.03 (m, 1 H, $C_\beta H_{Phe}$), 2.99 (m, 1 H, $C_\beta H_{Phe}$), 1.32 (d, $^3J_{H,H}$ = 7.2 Hz, 3 H, $CH_{3,Ala}$). ^{13}C NMR ([D$_6$]DMSO, 125.8 MHz): δ = 231.2, 230.3 (CO), 172.4, 171.8 ($C{=}O_{ester}$ + $C{=}O_{Ala}$), 165.6 (C=O), 158.8, 150.0, 137.5, 137.0, 135.4, 134.0, 131.4, 129.1, 128.2, 127.5, 126.5, 123.0, 122.3 (C_{Ar}), 68.9 ($CH_{2,Bz}$), 64.2 (CH_2), 53.6, 51.8 ($C_{\alpha,Phe}$ and OCH_3), 48.6 ($C_{\alpha,Ala}$), 36.6 ($C_{\beta,Phe}$), 17.7 ($CH_{3,Ala}$).

X-ray Crystallography: Transparent yellow single crystals of **1** and **2** were coated with perfluoropolyether, picked up with glass fibres and mounted on a Nonius Kappa-CCD diffractometer, equipped with a rotating Mo anode setup. An orange/yellow crystal of **4** was mounted on a Siemens SMART diffractometer with a sealed X-ray tube. Both diffractometers were equipped with graphite monochromators [λ(Mo-K_α) = 0.71073 Å] and a cryogenic nitrogen stream operating at 100(2) K. Crystallographic data of the compounds are listed in Table 6. Cell constants were obtained from a least-squares fit of the diffraction angles of several thousand strong reflections. Intensity data were corrected for Lorentz and polarisation effects. Crystal faces of **4** were determined and the face-indexed correction routine embedded in SHELXTL[41] was used to account for absorption, giving minimum and maximum transmission factors of 0.642 and 0.882. Intensity data of **2** were corrected by use of the

Table 6. Crystallographic data for **1**, **2**, and **4**

Compound	**1**	**2**	**4**
Empirical formula	$C_{15}H_{13}MoN_3O_3$	$C_{22}H_{19}MoN_3O_3$	$C_{24}H_{26}BrF_6Mo_2N_6O_4P$
Formula mass	379.22	469.34	879.27
Crystal size [mm]	0.27 × 0.18 × 0.10	0.22 × 0.06 × 0.03	0.50 × 0.30 × 0.06
Crystal system	orthorhombic	monoclinic	monoclinic
Space group	$Pna2_1$	Cc	$P2_1/n$
a [Å]	15.347(3)	7.1786(3)	13.0262(9)
b [Å]	8.449(2)	32.6222(5)	9.4274(7)
c [Å]	22.454(4)	17.2691(8)	24.258(2)
β [°]	90	96.09(2)	99.15(2)
V [Å^3]	2911.5(10)	4021.3(4)	2941.1(4)
Z	8	8	4
ρ (calcd.) [g/cm^3]	1.730	1.550	1.986
Absorption coefficient [mm^{-1}]	0.917	0.681	2.347
F(000)	1520	1904	1728
T [K]	100(2)	100(2)	100(2)
θ range for data collection [°]	2.58−23.99	2.37−32.50	1.67−32.50
Reflections collected	13280	32679	30836
Independent reflections/R(int)	3516/0.1324	12102/0.0738	10168/0.0354
Observed reflections [$I > 2\sigma(I)$]	2557	10853	8030
Data/restraints/parameters	3487/1/397	12077/2/523	10168/0/397
$R1$[a] /$wR2$[b](obsd. data)	0.0559/0.1269	0.0389/0.0913	0.0324/0.0732
$R1$[a] and $wR2$[b] (all data)	0.1024/0.2085	0.0522/0.1213	0.0493/0.0781
Goodness-of-fit on F^2 [c]	1.063	1.009	0.998
Largest diff. peak/hole [e/Å^3]	1.018/−1.038	0.764/−1.577	1.326/−0.843

[a] $R1 = \Sigma||F_o| - |F_c||/\Sigma|F_o|$. [b] $wR2 = [\Sigma[w(F_o^2 - F_c^2)^2]/\Sigma[w(F_o^2)_2]^{1/2}$, where $w = 1/\sigma^2(F_o^2) + (aP)^2 + bP$, $P = (F_o^2 + F_c^2)/3$. [c] GooF = $\{\Sigma[w(F_o^2 - F_c^2)^2]/(n - p)\}^{1/2}$, where n = no. of refl. and p = number of refined parameters.

semiempirical correction program MULSCANABS, part of the PLATON99[66] program suite, giving transmission factors of 0.757 and 0.944. Intensity data of **1** were left uncorrected. The Siemens SHELXTL[41] software package was used for solution, refinement, and depiction of the structures, and neutral atom scattering factors of the program were used. Non-hydrogen atoms were refined anisotropically, and hydrogen atoms were placed at calculated positions and refined as riding atoms with isotropic displacement parameters. CCDC-168208 (**1**), -168209 (**2**) and -168210 (**4**) contain the supplementary crystallographic data for this paper. These data can be obtained free of charge at www.ccdc.cam.ac.uk/conts/retrieving.html or from the Cambridge Crystallographic Data Centre, 12, Union Road, Cambridge CB2 1EZ, UK [Fax: (internat.) + 44-1223/336-033; E-mail: deposit@ccdc.cam.ac.uk].

Acknowledgments

The experimental work described in this article was carried out at the Max-Planck-Institut für Strahlenchemie. The authors are grateful to Professor K. Wieghardt for generous support of our work and to Professor P. Chaudhuri for many helpful discussions. Dr. E. Bill is thanked for his help with the EPR spectroscopic data acquisition and interpretation. Kerstin Sand and Jörg Bitter are kindly acknowledged for recording the NMR spectra. Heike Schucht and Petra Höfer are thanked for their technical assistance with the X-ray crystal structure determination and spectro-electrochemical measurements, respectively. This work was supported financially by the Fond der Chemischen Industrie and a Karl-Ziegler fellowship (N. M.-N.).

[1] G. Jaouen, A. Vessières, I. S. Butler, *Acc. Chem. Res.* **1993**, *26*, 361−369.
[2] M. Salmain, A. Vessières, P. Brossier, I. S. Butler, G. Jaouen, *J. Immun. Meth.* **1992**, *148*, 65−75.
[3] N. Metzler-Nolte, *Angew. Chem.* **2001**, *113*, 1072−1076; *Angew. Chem. Int. Ed.* **2001**, *40*, 1040−1043.
[4] A. Vessières, M. Salmain, P. Brossier, G. Jaouen, *J. Pharm. Biomed. Anal.* **1999**, *21*, 625−633.
[5] R. L. Cox, T. D. Schneider, M. D. Koppang, *Anal. Chim. Acta* **1992**, *262*, 145−159.
[6] H. Eckert, M. Koller, *J. Liq. Chromatogr.* **1990**, *13*, 3399−3414.
[7] D. R. van Staveren, T. Weyhermüller, N. Metzler-Nolte, *Organometallics* **2000**, *19*, 3730−3735.
[8] D. R. van Staveren, E. Bill, E. Bothe, T. Weyhermüller, M. Bühl, N. Metzler-Nolte, *Chem. Eur. J.*, in print.
[9] D. R. van Staveren, E. Bothe, T. Weyhermüller, N. Metzler-Nolte, *Chem. Commun.* **2001**, 131−132.
[10] D. D. Cox, S. J. Benkovic, L. M. Bloom, F. C. Bradley, M. J. Nelson, L. Que, Jr., D. E. Wallick, *J. Am. Chem. Soc.* **1988**, *110*, 2026−2032.
[11] N. Niklas, O. Walter, R. Alsfasser, *Eur. J. Inorg. Chem.* **2000**, 1723−1731.
[12] D. R. van Staveren, Ph.D. Thesis (Doktorarbeit), Ruhr-Universität, Bochum, **2001**.
[13] J. K. Romary, J. D. Barger, J. E. Bunds, *Inorg. Chem.* **1968**, *7*, 1142−1145.

[14] B. de Bruin, J. A. Brands, J. J. J. M. Donners, M. P. J. Donners, R. de Gelder, J. M. M. Smits, A. W. Gal, A. L. Spek, *Chem. Eur. J.* **1999**, *5*, 2921−2936.
[15] H. A. Jenkins, G. P. A. Yap, R. J. Puddephatt, *Organometallics* **1997**, *16*, 1946−1955.
[16] B. J. Brisdon, M. Cartwright, A. G. W. Hodson, M. F. Mahon, K. C. Molloy, *J. Organomet. Chem.* **1992**, *435*, 319−335.
[17] H. Kelm, H.-J. Krüger, *Eur. J. Inorg. Chem.* **1998**, 1381−1385.
[18] M. Rossignoli, P. V. Bernhardt, G. A. Lawrance, *J. Chem. Soc., Dalton Trans.* **1997**, 4247−4250.
[19] S. P. van Kouwenberg, E. H. Wong, G. R. Weisman, E. J. Gabe, F. L. Lee, P. Jackson, *Polyhedron* **1989**, *8*, 2333−2338.
[20] F. A. Cotton, G. A. Rusholme, A. Shaver, *J. Coord. Chem.* **1973**, *3*, 99−104.
[21] K.-B. Shiu, J. Y. Lee, Y. Wang, M.-C. Cheng, S.-L. Wang, F.-L. Liao, *J. Organomet. Chem.* **1993**, *453*, 211−219.
[22] C. P. Marabella, J. H. Enemark, *J. Organomet. Chem.* **1982**, *226*, 57−62.
[23] T. J. Desmond, F. J. Lalor, G. Ferguson, M. Parvez, *J. Organomet. Chem.* **1984**, *277*, 91−97.
[24] I. T. MacLeod, E. R. T. Tiekink, C. G. Young, *J. Organomet. Chem.* **1996**, *506*, 301−306.
[25] G. Haselhorst, S. Stoetzel, A. Strassburger, W. Walz, K. Wieghardt, B. Nuber, *J. Chem. Soc., Dalton Trans.* **1993**, 83−90.
[26] N. L. Armanasco, M. V. Baker, M. R. North, B. W. Skelton, A. H. White, *J. Chem. Soc., Dalton Trans.* **1998**, 1145−1149.
[27] A. Chandrasekeran, S. S. Krishnamurthy, M. Nethaji, *Curr. Sci.* **1991**, *60*, 700−701.
[28] A. Chandrasekeran, S. S. Krishnamurthy, M. Nethaji, *J. Chem. Soc., Dalton Trans.* **1994**, 63−68.
[29] G. G. Aleksandrov, V. N. Babin, A. P. Kharchenikov, Y. T. Struchkov, N. S. Kochetkova, *J. Organomet. Chem.* **1984**, *266*, 109−116.
[30] C.-Y. Kuo, Y.-S. Fuh, J.-Y. Shiue, S. J. Yu, G.-H. Lee, S.-M. Peng, *J. Organomet. Chem.* **1999**, *588*, 260−267.
[31] R. W. Hay, I. Fraser, G. Ferguson, *J. Chem. Soc., Chem. Commun.* **1987**, 1715−1716.
[32] R. W. Hay, I. Fraser, G. Ferguson, *J. Chem. Soc., Dalton Trans.* **1989**, 2183−2186.
[33] T. M. Bockman, J. K. Kochi, *New J. Chem.* **1992**, *16*, 39−49.
[34] F. A. Cotton, R. M. Wing, *Inorg. Chem.* **1965**, *4*, 314−317.
[35] P. Chaudhuri, K. Wieghardt, Y.-H. Tsai, C. Krüger, *Inorg. Chem.* **1984**, *23*, 427−432.
[36] K. Wieghardt, M. Hahn, W. Swiridoff, J. Weiss, *Angew. Chem.* **1983**, *95*, 499−500; *Angew. Chem. Int. Ed. Engl.* **1983**, *22*, 491−492.
[37] R. Hazama, K. Umakoshi, A. Ichimura, S. Ikari, Y. Sasaki, T. Ito, *Bull. Chem. Soc. Jpn.* **1995**, *68*, 456−468.
[38] A. Kojima, S. Ooi, Y. Sasaki, K. Z. Suzuki, K. Saito, H. Kuroya, *Bull. Chem. Soc. Jpn.* **1981**, *54*, 2457−2465.
[39] K. Z. Suzuki, Y. Sasaki, S. Ooi, K. Saito, *Bull. Chem. Soc. Jpn.* **1980**, *53*, 1288−1298.
[40] H. Günther, *NMR Spectroscopy*, John Wiley & Sons, New York, **1980**.
[41] *SHELXTL V. 5*, Siemens Analytical X-ray Instruments, Inc. **1994**.
[42] M. Minelli, J. H. Enemark, R. T. C. Brownlee, M. J. O'Connor, A. G. Wedd, *Coord. Chem. Rev.* **1985**, *68*, 169−278.
[43] D. Rehder, *Coord. Chem. Rev.* **1991**, *110*, 161−210.
[44] R. T. C. Brownlee, M. J. O'Connor, B. P. Shehan, A. G. Wedd, *J. Magn. Res.* **1985**, *64*, 142−144.
[45] K. Wieghardt, M. Gutmann, P. Chaudhuri, W. Gebert, M. Minelli, C. G. Young, J. H. Enemark, *Inorg. Chem.* **1985**, *24*, 3151−3155.
[46] A. F. Masters, R. T. C. Brownlee, M. J. O'Connor, A. G. Wedd, J. D. Cotton, *J. Organomet. Chem.* **1980**, *195*, C17−C20.
[47] E. C. Alyea, A. Somogyvari, in: H. F. Barry, P. C. H. Mitchell (Eds.), *Proceedings of the Climax Fourth International Conference on the Chemistry and Uses of Molybdenum*, Climax Molybdenum Company, Ann Arbor, MI, **1982**, p. 46.
[48] G. Backes-Dahmann, W. Herrmann, K. Wieghardt, J. Weiss, *Inorg. Chem.* **1985**, *24*, 485−491.
[49] J. H. MacNeil, A. W. Roszak, M. C. Baird, K. F. Preston, A. L. Rheingold, *Organometallics* **1993**, *12*, 4402−4412.
[50] T. Beissel, B. S. P. C. Della Vedova, K. Wieghardt, R. Boese, *Inorg. Chem.* **1990**, *29*, 1736−1741.
[51] S. Trofimenko, *J. Am. Chem. Soc.* **1969**, *91*, 588−595.
[52] M. D. Curtis, K.-B. Shiu, W. M. Butler, J. C. Huffman, *J. Am. Chem. Soc.* **1986**, *108*, 3335−3343.
[53] K.-B. Shiu, L.-Y. Lee, *J. Organomet. Chem.* **1988**, *348*, 357−360.
[54] M. D. Curtis, K.-B. Shiu, *Inorg. Chem.* **1985**, *24*, 1213.
[55] M. Savignac, A. Sasaki, P. Potier, G. Jaouen, *J. Chem. Soc., Chem. Commun.* **1991**, 615−617.
[56] B. El Mouatassim, H. Elamouri, J. Vaissermann, G. Jaouen, *Organometallics* **1995**, *14*, 3296−3302.
[57] D. Osella, M. Ravera, M. Vincenti, M. Salmain, G. Jaouen, *Organometallics* **1996**, *15*, 3037−3041.
[58] A. Gorfti, M. Salmain, G. Jaouen, *J. Chem. Soc., Chem. Commun.* **1994**, 433−434.
[59] A. Gorfti, M. Salmain, G. Jaouen, M. J. McGlinchey, A. Bennouna, A. Mousser, *Organometallics* **1996**, *15*, 142−151.
[60] M. Salmain, M. Gunn, A. Gorfti, S. Top, G. Jaouen, *Bioconjugate Chem.* **1993**, *4*, 425−433.
[61] A. Varenne, A. Vessières, S. M. S. Durand, P. Brossier, G. Jaouen, *Anal. Biochem.* **1996**, *242*, 172−179.
[62] M. Salmain, A. Vessières, A. Varenne, P. Brossier, G. Jaouen, *J. Organomet. Chem.* **1999**, *589*, 92−97.
[63] E. Bill, *GFIT*, unpublished.
[64] S. Dick, A. Weiss, *Z. Naturforsch., Teil B* **1997**, *52*, 188−192.
[65] G. J. Kubas, L. S. van der Sluys, *Inorg. Synth.* **1990**, *28*, 29−33.
[66] A. L. Spek, *PLATON, A Multipurpose Crystallographic Tool*, Utrecht University, Utrecht, The Netherlands, **1999**.

Received August 14, 2001
[I01310]